JTTEE5 6:361-367

Thermal and Mechanical Properties of ZrO_2-CeO_2 Plasma-Sprayed Coatings

S. Sodeoka, M. Suzuki, K. Ueno, H. Sakuramoto, T. Shibata, and M. Ando

The thermal and mechanical properties of ZrO_2-CeO_2 plasma-sprayed coatings were evaluated to examine their potential as a thermal barrier coating. ZrO_2-CeO_2 solid-solution powders containing up to 70 mol% CeO_2 are successfully plasma sprayed, but cerium content decreases during spraying due to the vaporization of cerium oxide. Hardness is greatest at 30 mol% CeO_2. With increased CeO_2 content, the thermal conductivity decreases to 0.5 W/m · K and the thermal expansion coefficient increases to 12.5 × 10^{-6}/K. Increased torch input power causes both the relative density and the hardness to increase monotonically, while the thermal conductivity and the thermal expansion coefficient are not significantly affected. When heated above 1300 K, the coating shrinks considerably due to sintering and its thermal conductivity increases abruptly.

Keywords ceria stabilization, processing parameters, thermal barrier coating

1. Introduction

Plasma-sprayed thermal barrier coating (TBC) is applied to hot sections in gas turbines or jet engines, such as a combustor can, nozzle guide vanes, and turbine blades. The aim is to increase engine efficiency by elevating the operational temperature or reducing cooling air. The coating enables extension of component life by lowering the metal temperature. The development of high-performance TBCs for higher-temperature use is being driven by the demand for higher fuel efficiency.

Zirconia (ZrO_2)-based coatings are commonly used as TBCs because of their low thermal conductivity and high coefficient of thermal expansion (Ref 1, 2). The good mechanical properties of plasma-sprayed zirconia, partially stabilized with yttria (Y_2O_3), contribute to its wide use, especially in aerospace applications (Ref 1, 3, 4).

Ceria (CeO_2) has lower thermal conductivity and a higher thermal expansion coefficient than zirconia (Ref 5). It is also known that ceria-stabilized zirconia exhibits high fracture toughness (Ref 6). Therefore, the combination of CeO_2 and ZrO_2 can be expected to produce advanced TBCs with high heat-shielding capacity and high fracture resistance. However, published reports dealing with ceria-containing TBCs are limited (Ref 7-9). No data on the thermal and mechanical properties of ceria-stabilized zirconia coating containing more than 25 mol% CeO_2 have been reported. The objective of this paper is to clarify the thermal and mechanical properties of ZrO_2-CeO_2 plasma-sprayed coatings containing a large amount of cerium and to examine their potential as TBCs.

S. Sodeoka, M. Suzuki, and **K. Ueno,** Osaka National Research Institute, Agency of Industrial Science and Technology, Midorigaoka 1-8-31, Ikeda, Osaka, 563, Japan; **H. Sakuramoto, T. Shibata,** and **M. Ando,** Osaka Electronics and Communication University, Hatsucho 18-8, Neyagawa, Osaka, 572, Japan.

2. Experimental

2.1 *Powder Preparation*

Spray powder was prepared from commercially available zirconium oxide powder (TZ-0Y, Tosoh Co., Tokyo; purity > 99.9%) and cerium oxide powder (H.C.CeO_2, Santoku-Metal Co. Ltd., Kobe; purity > 99.9%). These powders were mixed by ball milling in ethyl alcohol to obtain five types of powder mixtures with CeO_2 contents of 0, 30, 50, 70, and 100 mol%, respectively. After drying, each powder mixture was die pressed at 29.4 MPa, fired at 1873 K for 5 h in air to make a solid solution, and crushed to a particle size smaller than 1 μm by a planetary ball mill. This process was repeated three times until the x-ray diffraction (XRD) pattern no longer changed. Spherically granulated powder was made by spray drying with polyvinyl alcohol as a binder and classified between 25 and 45 μm.

Table 1 Spraying parameters

Test objective	Gun	Plasma gas: Argon m³/s	Plasma gas: Argon L/min	Plasma gas: H_2 m³/s	Plasma gas: H_2 L/min	Input power kW	Input power A	Spray distance, mm	Feed rate kg/s	Feed rate g/min
Investigate effect of composition	Metco 9MB	7.0×10^{-4}	42	1.4×10^{-4}	8.2	36	600	75	5×10^{-4}	30
Examine effect of torch input power	Metco 9MB	7.0×10^{-4}	42	$1.2\text{-}1.4 \times 10^{-4}$	7-8.2	36, 42, 48, 54	600, 700, 800, 900	75	5×10^{-4}	30
Test properties at high temperature	Metco 9MB	7.0×10^{-4}	42	1.2×10^{-4}	7	48	800	75	5×10^{-4}	30

2.2 *Plasma Spraying*

Plasma spraying was carried out with a Metco 9MB gun (Sulzer Metco, Westbury, NY) in air. Argon gas was the primary plasma gas, and hydrogen gas was added as the secondary gas. Spraying parameters are shown in Table 1. The substrate was carbon steel (JIS-SS400) that was blasted with 24-mesh alumina grit just prior to spraying. The sprayed coating was formed directly on the substrate, with no bond coating. The deposit and the substrate were cooled by air blowing onto the surface and by use of a water-cooled specimen holder.

2.3 *Coating Evaluation*

Deposition efficiency was defined as a ratio of the deposit weight to the amount of fed powder. Spraying was directed onto the center of the 100 by 100 by 3 mm substrate for 60 s without gun traverse.

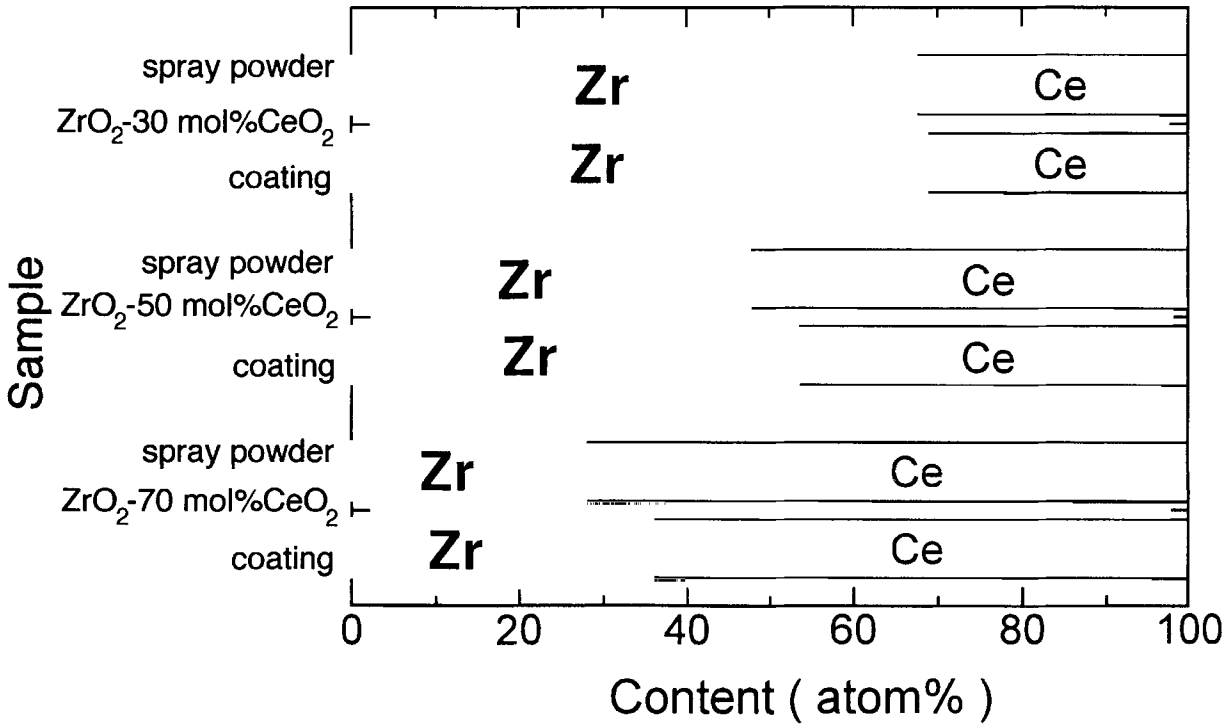

Fig. 1 Change in composition of ZrO_2-CeO_2 by plasma spraying. Upper bar, spray powder; lower bar, coating

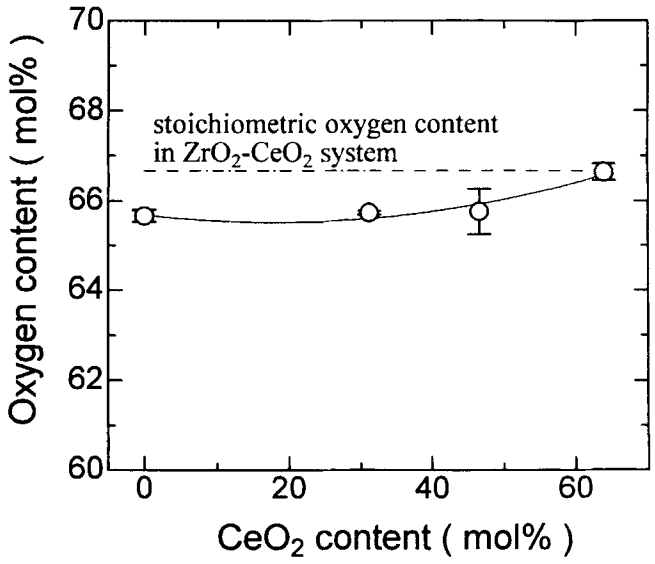

Fig. 2 Variation in oxygen content of ZrO_2-CeO_2 coating with CeO_2 content

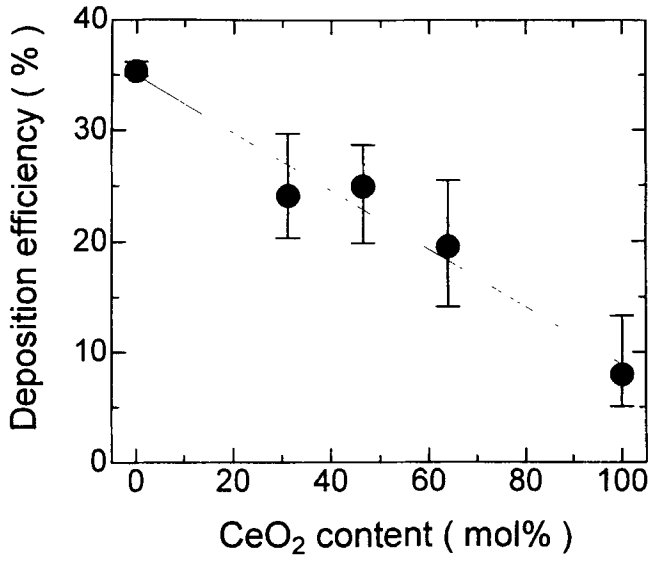

Fig. 3 Variation in deposition efficiency of ZrO_2-CeO_2 coating with CeO_2 content

Bulk density was measured by the water-immersion method using a free-standing deposit separated from the substrate by etching with hydrochloric acid. Relative density was determined by dividing the bulk density by the true density, which was measured by the pycnometer method with the pulverized deposit. Crystallographic phases were determined by XRD. The content of metallic elements in the powders and the coatings was measured quantitatively by x-ray fluorescence analysis. Oxygen content was determined using a nitrogen-oxygen analyzer (EMGA-2800; Horiba Ltd., Kyoto). Vickers microhardness (HV) was measured on polished cross section with an indentation load of 2.94 N for 15 s. Thermal conductivity (λ) along the direction perpendicular to the coating surface was measured by the laser-flash method. The thermal expansion coefficient (α) was measured by a differential dilatometer using alumina as a reference.

3. Results and Discussion

3.1 *Effect of Powder Composition*

Figure 1 shows the Zr/Ce ratios in the spray powders and the coatings measured by x-ray fluorescence analysis. Cerium content decreased after spraying in each composition. The cerium decrease was greater in the cerium-rich composition. This decreased cerium content was probably due to the decomposition and vaporization of CeO_2 by overheating during spraying. Also, some CeO_2 may possibly be reduced to Ce_2O_3 in an Ar-H_2 plasma. Though CeO_2 melts at about 3023 K, a rather higher melting point than that of ZrO_2 (2988 K), Ce_2O_3 melts at 1963 K (Ref 10). These facts suggest that Ce_2O_3 was heated to a temperature far higher than its melting point when the ZrO_2-CeO_2 system was successfully sprayed. Such superheating inevitably results in the vaporization of Ce_2O_3 and in the selective decrease in cerium.

Spraying with Ar-H_2 plasma also caused the oxygen content to become lower than the stoichiometric content in the ZrO_2-CeO_2 system, as indicated by the broken line in Fig. 2. The oxygen loss is greatest in the pure ZrO_2 coating, where about 1.5% of the oxygen sites are vacant, and decreases with an increase in CeO_2 content. In this paper, CeO_2 content, which is often used as the horizontal axis of graphs, was determined from the Ce/Zr atomic ratio by neglecting any oxygen loss.

Deposition efficiency decreased with increased CeO_2 content (Fig. 3). It is known that the efficiency is generally affected by various factors, including improper powder feeding into the plasma flame. In our case, the main cause of the efficiency decrease with increasing CeO_2 content may be the vaporization of CeO_2. Judging from the decrease of cerium (see Fig. 1), the weight loss by vaporization during spraying is estimated at 2.0, 12.7, and 24.3 mass% for 30, 50, and 70 mol% CeO_2 powder, respectively. The deposition efficiency of pure CeO_2 was lower than 10%, which is less than those of other systems. The deposit was so friable that property evaluations could only be made by XRD.

Figure 4 shows the variations in bulk density and relative density of the coating with CeO_2 content. Because of the heavy atomic weight of cerium, the bulk density increased with CeO_2 content. On the other hand, the relative density decreased with addition of CeO_2; the relative densities of ZrO_2 and ZrO_2-CeO_2 coatings were 92.4%, and 88 to 89%, respectively. These results for spraying efficiency and coating density suggest that CeO_2 incorporation makes it difficult to fabricate dense coatings by thermal spraying.

X-ray diffraction profiles are shown in Fig. 5(a) and (b). The ZrO_2 coating was composed of monoclinic phase only, the ZrO_2-CeO_2 coatings contained both tetragonal and cubic phases, and the CeO_2 coating was composed of cubic phase (Fig. 5a). These results were in good agreement with the equilibrium phase diagram (Ref 11). When the diffraction profiles of these coatings were compared with those of spray powders, there were no remarkable changes except for a small shift of the peak position owing to the change in cerium content. Detailed examination of the ZrO_2-CeO_2 coatings (Fig. 5b) revealed that the fraction of cubic phase increased in proportion to CeO_2 content. Furthermore, the shifts of the peaks to low angles suggest that the lattice size increased with increasing CeO_2 content for both the cubic and the tetragonal phases.

The variation in Vickers microhardness (HV) with CeO_2 content is shown in Fig. 6. Addition of 30 mol% CeO_2 increased HV slightly compared to ZrO_2 coating despite the significant decrease in relative density. Since CeO_2 is a softer material than ZrO_2 (Ref 5), the hardness is probably affected by the fracture resistance enhanced by the stress-induced transformation of the tetragonal phase that was formed by incorporation of CeO_2. The cerium addition of more than 40 mol% caused the hardness degradation. As the relative densities of these coatings are comparable to that of 30 mol% Ce coating, the decrease in hardness probably depends on the decrease in the tetragonal phase. Weaker bond strength of Ce-O as compared with that of Zr-O may also contribute to this hardness decrease (Ref 12).

Figure 7 shows the variation in average thermal expansion coefficient (α) from room temperature to 1073 K (open circle) and thermal conductivity (λ) at room temperature (solid circle) with CeO_2 content. The thermal expansion coefficient of CeO_2-containing coatings became one and a half times as large as that or pure ZrO_2 coating. Monoclinic single-crystal ZrO_2 is reported to have an α value of 8.1×10^{-6}/K (298 to 1453 K) (Ref

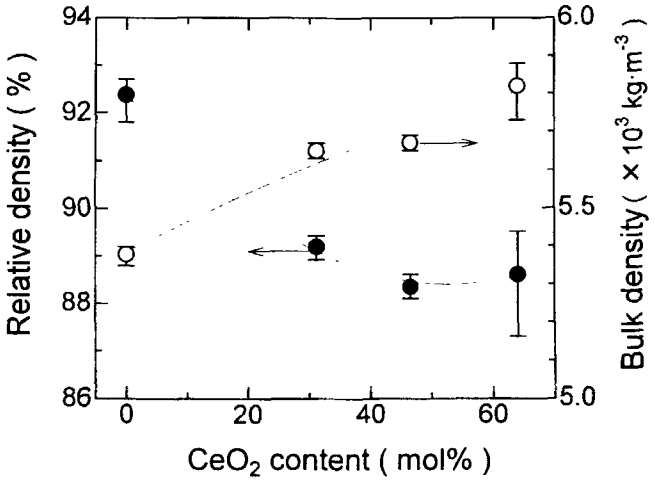

Fig. 4 Variations in bulk density (open circles) and relative density (solid circles) of ZrO_2-CeO_2 coating with CeO_2 content

13), whereas CeO_2 has an α value of 13.4×10^{-6}/K (273 to 1473 K) (Ref 5). The tendency shown in Fig. 7 corresponds well to these data. It is notable that α does not depend on the CeO_2 content in the ZrO_2-CeO_2 system.

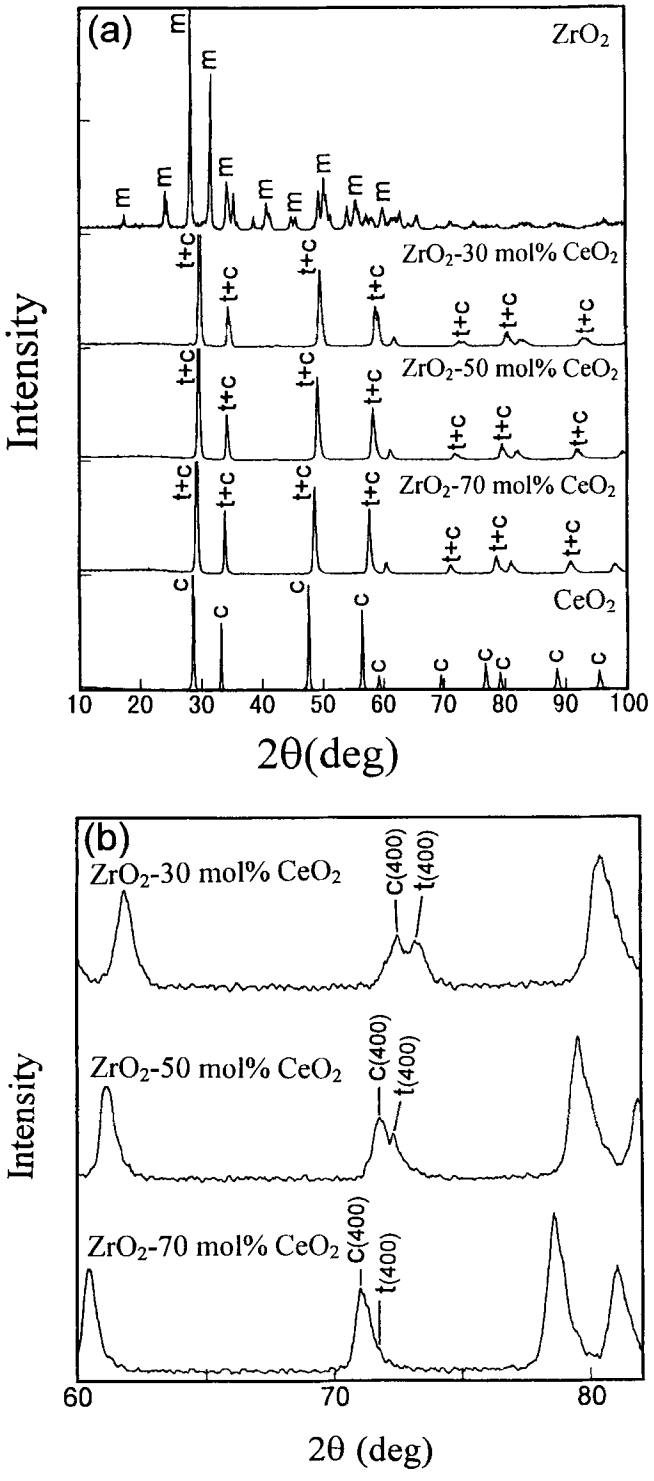

Fig. 5 XRD profiles of ZrO_2-CeO_2 coatings measured with Cu-Kα. (a) Wide-angle survey. (b) Detail indicating phase composition. c, cubic; m, monoclinic; t, tetragonal

Thermal conductivity decreased with increasing CeO_2 content. The curve is similar to that of the relative density (see Fig. 4), suggesting the strong influence of porosity on λ. However, as described later, the relative density has little influence on λ of coatings with the same composition. The decrease in λ, therefore, reflects the material property. In ceramics, which behave as insulators, λ is generally controlled by the lattice vibration (Ref 14). Thus, λ becomes lower when the material is composed of the solid solution of elements with different atomic weights and ion radii. A heavy atomic weight or large ion radius of the element also decreases λ. In this work, ZrO_2-CeO_2 is a solid solution and cerium has a heavier atomic weight and larger ion radius than zirconium; thus, CeO_2 addition reduces λ.

3.2 *Effect of Torch Input Power*

The effect of torch input power on the properties of the coating from ZrO_2-50 mol% CeO_2 powder was examined. Plasma spraying was carried out with four levels of input power—36, 42, 48, and 54 kW—by controlling the electric current from 600 to 900 A. In the coating sprayed at 54 kW, some cracks perpendicular to the surface were observed, probably due to overheating.

With plasma spraying, the cerium content decreased to about 43 at.% in each coating and no significant difference due to torch input power was observed. The XRD result indicates no distinctive difference in crystallographic phases due to the power level. All coatings were partially stabilized with tetragonal and cubic phases.

The variations in relative density and Vickers hardness with input power are shown in Fig. 8. Relative density increased monotonously from 88.2% (at 36 kW) to 90.4% (at 54 kW) with an increase in power, as generally seen in plasma spraying with ceramics. Corresponding to the density, Vickers hardness increased to 5.5 GPa at 54 kW with an increase in power.

The average thermal expansion coefficient from room temperature to 1073 K was about 12×10^{-6}/K at any input power.

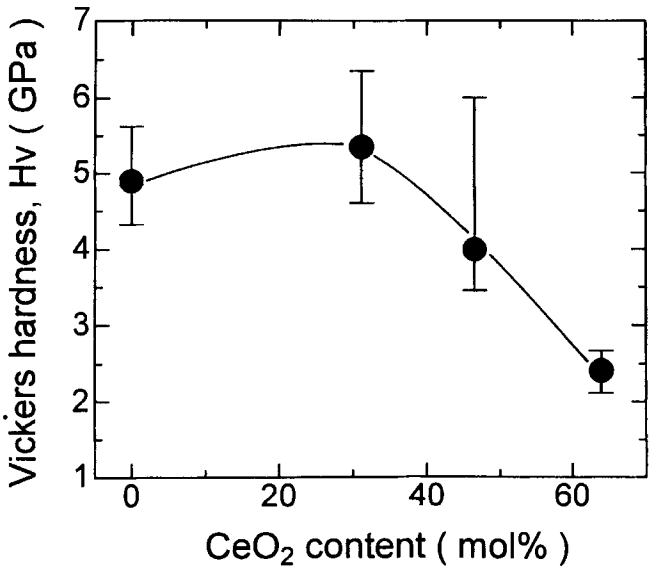

Fig. 6 Variation in Vickers microhardness of ZrO_2-CeO_2 coating with CeO_2 content

This value is not sensitive to the coating microstructure but strongly reflects the material property itself. Thermal conductivity (λ) at room temperature also showed almost the same value of about 0.5 W/m · K for all coatings fabricated under various input powers. In principle, this value is known to be affected by porosity (Ref 15). In this work, the relative density was changed by input power but λ was not influenced, probably because of the peculiar structure of a sprayed coating. Plasma-sprayed ceramic coatings are composed of piles of flattened particles, and the area fraction of adhesion between the particles is reported as 30% (Ref 16). The gap between particles, which does not contribute to the heat conduction, occupies 70% of area and makes the effect of porosity negligible. This may also be the reason why a sprayed coating shows much lower thermal conductivity than the sintered bulk.

For example, the λ value of a sintered sample of CeO_2-40 mass% (ZrO_2-4 mol% Y_2O_3) is about 2.4 W/m · K (Ref 12), in which CeO_2 content corresponds to 52 mol% and 2% porosity is included. This value is five times higher than that of ZrO_2-50 mol% CeO_2 coating (0.5 W/m · K). If the fraction of heat-conductive area is also about 30% in our ZrO_2-CeO_2 coating, a simple estimation of effective thermal conductivity is 0.72 W/m · K (= 2.4 W/m · K × 0.3), indicating good agreement with the measured value.

3.3 *Properties at Elevated Temperature*

In order to investigate the stability of ZrO_2-CeO_2 coating at elevated temperature, heat treatments at 1573, 1673, and 1773 K were carried out and changes in coating properties were examined. Thermal conductivity from room temperature to 1773 K was also measured.

The change in the bulk density of ZrO_2-50 mol% CeO_2 coating by the heat treatment is shown in Fig. 9. At each temperature, the density increased rapidly within 20 h and then changed very little up to 100 h. The higher the treatment temperature, the higher the final density. Microstructures of coatings as-sprayed and heat treated at 1773 K are shown in Fig. 10. The as-sprayed coating shows a lamellar structure composed of flattened particles, typical of sprayed deposits. In contrast, the heat-treated coating shows a structure like a sintered body with equiaxial grains and spherical pores. This indicates that the density increase was caused by sintering.

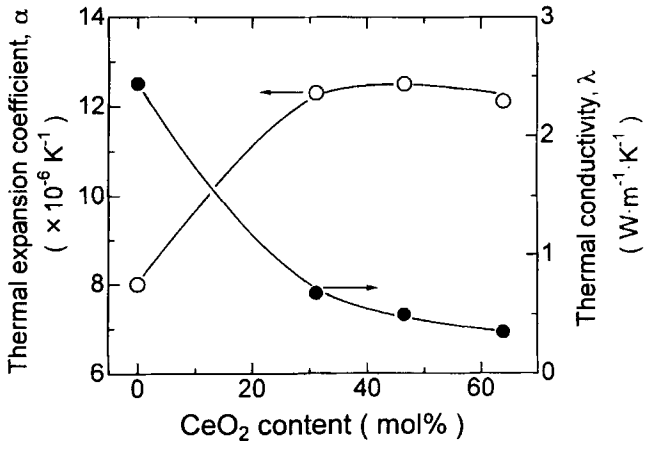

Fig. 7 Variations in average thermal expansion coefficient from room temperature to 1073 K (open circles) and thermal conductivity at room temperature (solid circles) of ZrO_2-CeO_2 coating with CeO_2 content

With plasma spraying, the CeO_2 content decreased as mentioned in section 3.1. It decreased further when heat treated above 1573 K.

The variation of thermal conductivity of ZrO_2-50 mol% CeO_2 coating with temperature up to 1773 K is shown in Fig. 11. The value decreased gradually up to 1300 K, above which it increased abruptly. The reason for this increase is probably that the

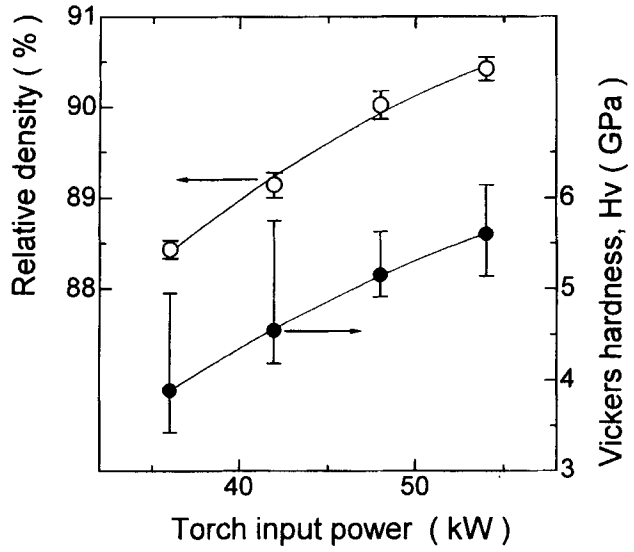

Fig. 8 Variations in relative density (open circles) and Vickers microhardness (solid circles) of ZrO_2-50 mol% CeO_2 coating with input power

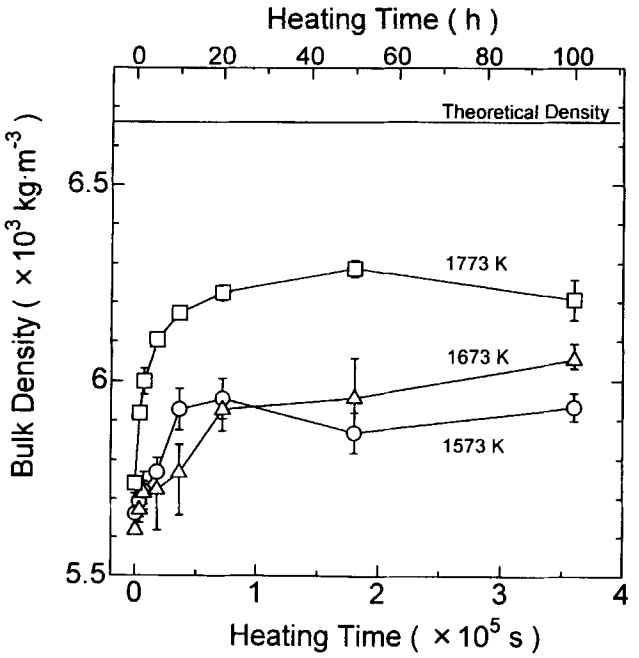

Fig. 9 Variation in bulk density of ZrO_2-50 mol% CeO_2 coating by heat treatment

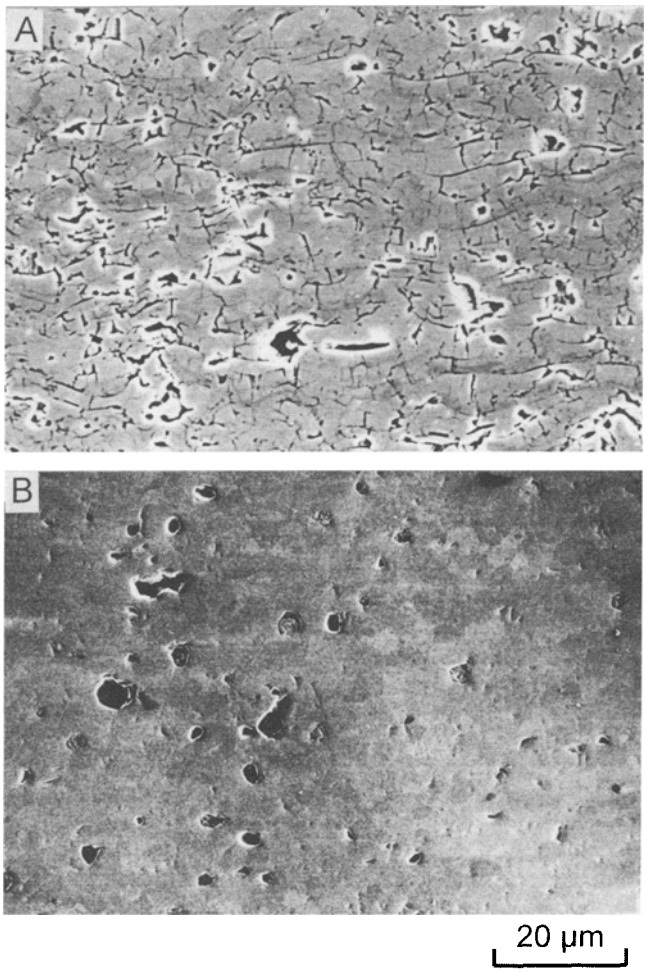

Fig. 10 Cross-sectional microstructures of ZrO_2-50 mol% CeO_2 coatings. (a) As-sprayed. (b) Heat treated at 1773 K

narrow spaces between lamellae, which prevent heat flow, vanish gradually during sintering. On the other hand, the decrease up to 1300 K can be explained by an increase of phonon scattering due to enhanced lattice vibration with rising temperature, the same tendency reported in CeO_2 sintered ceramics (Ref 5).

4. Conclusions

The thermal and mechanical properties of ZrO_2-CeO_2 plasma-sprayed coatings were evaluated.

- ZrO_2-CeO_2 powder with CeO_2 content up to 70 mol% was successfully plasma sprayed, but CeO_2 content decreased during the spraying due to the vaporization of cerium oxide.
- The hardness of the ZrO_2-CeO_2 coating exhibited a maximum at 30 mol% CeO_2.
- Thermal conductivity decreased and the thermal expansion coefficient increased with an increase in CeO_2 content.
- With increased torch input power, both relative density and hardness increased monotonically, while thermal conductivity and the thermal expansion coefficient were not significantly affected.

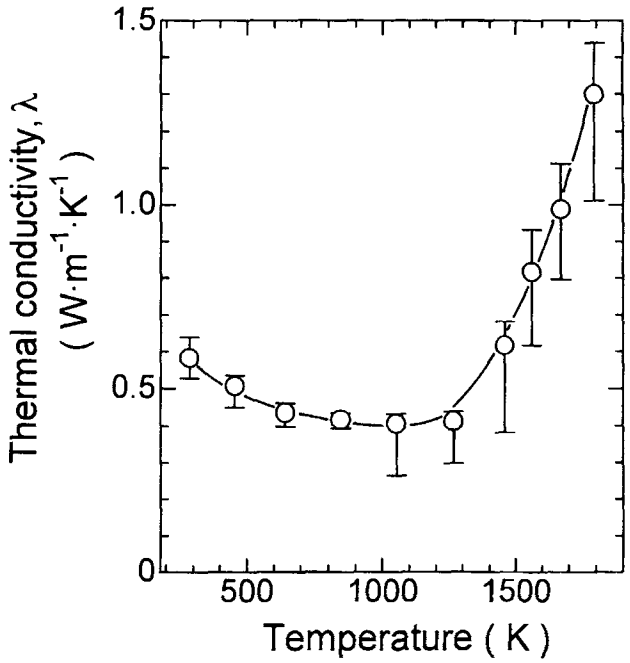

Fig. 11 Variation in thermal conductivity of ZrO_2-50 mol% CeO_2 coating with temperature

- When heated above 1300 K, the coating contracted due to sintering and its thermal conductivity increased abruptly.

From these results, it is concluded that CeO_2 addition to plasma-sprayed ZrO_2 coating effectively improves some properties for TBCs, resulting in low thermal conductivity and a thermal expansion coefficient close to that of the metal substrate. Improvement in high-temperature stability is desirable for practical use.

References

1. R.A. Miller, Current Status of Thermal Barrier Coatings—An Overview, *Surf. Coat. Technol.*, Vol 30, 1987, p 1-11
2. R.B. Brandt, L. Pawlowski, G. Neuer, and P. Fauchais, Specific Heat and Thermal Conductivity of Plasma Sprayed Yttria-Stabilized Zirconia and NiAl, NiCr, NiCrAl, NiCrAlY, NiCoCrAlY Coatings, *High. Temp.-High Press.*, Vol 18, 1986, p 65-77
3. M.F. Gruninger and M.V. Boris, Thermal Barrier Ceramics for Gas Turbine and Reciprocating Heat Engine Applications, *Thermal Spray: Advances in Coatings Technology*, D.L. Houck, Ed., ASM International, 1988, p 487-492
4. R. Sivakumar and B.L. Mordike, High Temperature Coatings for Gas Turbine Blades: A Review, *Surf. Coat. Technol.*, Vol 37, 1989, p 139-160
5. *Engineering Property Data on Selected Ceramics*, Vol III, *Single Oxides*, Metals and Ceramics Information Center, Battelle Columbus Laboratories, 1981, p 5.4.9-6
6. K. Tsukuma and M. Shimada, Strength, Fracture Toughness and Vickers Hardness of CeO_2-Stabilized Tetragonal ZrO_2 Polycrystals (Ce-TZP), *J. Mater. Sci.*, Vol 20, 1985, p 1178-1184
7. A. Rouanet, G. Peraudeau, F. Sibieude, T. Priem, R Ranc, E. Rigal, et al., Chemical and Structural Characterization of Quenched Ceria (Yttria) Stabilized Zirconia or Hafnia Ceramics for Plasma Coatings,

Thermal Spraying: Current Status and Future Trends, A. Ohmori, Ed., High Temperature Society of Japan, 1995, p 507-512

8. J.W. Holmes and B.H. Pilsner, Cerium Oxide Stabilized Thermal Barrier Coatings, *Thermal Spray: Advances in Coatings Technology,* D.L. Houck, Ed., ASM International, 1988, p 259-270
9. T. Suzuki, H. Takeda, M. Itoh, and Y. Takahashi, Properties of Plasma Sprayed CeO_2-ZrO_2-Y_2O_3 Thermal Barrier Coating, *Yogyo-Kyokai-Shi (J. Ceram. Soc. Jpn.),* Vol 94 (No. 9), 1986, p 992-997 (in Japanese)
10. Y. Shiraki, Sintered Zirconia and Sintered Ceria, *Fine Ceramics,* Gihoudo-Shuppan, Tokyo, 1976, p 455, 545 (in Japanese)
11. E.M. Levin, C.R. Robbins, and H.F. McMurdie, in *Phase Diagrams for Ceramists,* M.K. Reser, Ed., American Ceramic Society, 1964, p 140
12. K. Ueno, S. Sodeoka, and M. Tsutsumi, Thermal and Mechanical Properties of CeO_2-4mol%Y_2O_3 Partially Stabilized ZrO_2 Ceramics, *J. Jpn. Therm. Spray. Soc.,* Vol 32 (No. 4), 1995, p 221-226 (in Japanese)
13. J.W Adams, H.H. Nakamura, R.P Ingel, and R.W. Rice, Thermal Expansion Behavior of Single-Crystal Zirconia, *J. Am. Ceram. Soc.,* Vol 68 (No. 9), 1985, p C228-C231
14. W D. Kingery, Thermal Conductivity of Crystal, *Introduction to Ceramics,* John Wiley & Sons, 1960, p 486-497
15. W.D. Kingery, Thermal Conductivity of Multiphase Bodies, *Introduction to Ceramics,* John Wiley & Sons, 1960, p 499-508
16. Y. Arata, A. Ohmori, and C. Li, Structure and Properties of Plasma Sprayed Alumina Coatings, *J. High Temp. Soc. Jpn.,* Vol 14 (No 5), 1988, p 220-233 (in Japanese)